

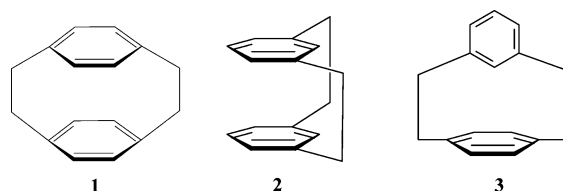
A Computational Study of [2.2]Cyclophanes

Giovanni F. Caramori,[†] Sérgio E. Galembek,^{*,†} and Kenneth K. Laali[‡]

Departamento de Química, FFCLRP, Universidade de São Paulo, 14040-901, Ribeirão Preto - SP, Brazil,
and Department of Chemistry, Kent State University, Kent, Ohio 44242

segalemb@usp.br

Received December 2, 2004



A computational study of isomeric [2.2]cyclophanes, namely [2.2]paracyclophane **1**, [2.2]metacyclophane **2**, and [2.2]metaparacyclophane **3**, has been carried out. For **1**, geometry optimizations performed by various methods at different basis sets showed that MP2/6-31+G(d,p) and B3PW91/6-31+G(d,p) provide the best results in comparison to the X-ray data. Compound **1** has D_2 symmetry with distorted bridges. A conformational search was performed for [2.2]cyclophanes **2** and **3**. Each cyclophane exists in two conformations which have different energies in the case of **3** but are degenerate in the case of **2**. Relative energies and strain energies at the bridges follow the same order, indicating that the relief of bridge tension and repulsion between π clouds are determining factors for the stability of [2.2]cyclophanes. Through a decomposition of strain energy, it can be concluded that both the rings or the bridges can absorb strain, but it depends on the conformer of butane that is considered in the calculation of SE(br). Changes in aromaticity of these compounds were evaluated by NICS and HOMA and were compared with benzene and xylenes dimers as models. Despite distortions from planarity and shortening and lengthening of the C–C bonds relative to the mean, the phenyl rings are aromatic. NICS suggests a concentration of electronic density between the rings as a result of bridging process. Computed MK, NPA, and GAPT charges were compared for the isomeric cyclophanes. The GIAO chemical shifts were calculated and indicate that **1** has a larger diamagnetic anisotropy than the other isomers.

1. Introduction

Cyclophanes have found application in several different areas, such as in asymmetric synthesis,¹ selective catalysis,² and supramolecular chemistry.³ They have also been utilized in various biorelated areas. For example, polymers prepared from cyclophanes by chemical deposition in the vapor phase (CVD)⁴ can form biomimetic layers with incorporated functional groups (proteins, antigens, cell receptors) which allows the control of the interactions between biomaterials and the organism.⁵

These compounds also act as selective synthetic receptors of anions that exhibit biological functions, e.g., carboxylates and phosphates.⁶

Over the years, [2.2]phanes, in particular, [2.2]-paracyclophane **1**, [2.2]metacyclophane **2**, and [2.2]metaparacyclophane **3** (Figure 1), have played a significant role in structural/mechanistic studies and served as valuable probes for understanding the interplay of aromaticity versus strain, transannular π - π interactions, and substituent effects.^{7–9} A number of X-ray structures have been published,⁷ and substantial data became available on their solution conformational studies. However, most of the available theoretical data on strain

* To whom correspondence should be addressed.

[†] Universidade de São Paulo.

[‡] Kent State University.

(1) Wörsdöfer, U.; Vögtle, F.; Nieger, M.; Waletzke, M.; Grimme, S.; Glorius, F.; Pfalts, A. *Synthesis* **2001**, 4, 597.

(2) Tabushi, I.; Yamamura, K. *Top. Curr. Chem.* **1983**, 113, 145.

(3) Jones, C. J. *Chem. Soc. Rev.* **1998**, 27, 289.

(4) Popova, E.; Antonov, D.; Sergeena, E.; Vonrotsov, E.; Stash, A.; Rozenberg, V.; Hopof, H. *Eur. J. Inorg. Chem.* **1998**, 1733.

(5) Lahan, J.; Höcker, H.; Langer, R. *Angew. Chem., Int. Ed.* **2001**, 40, 4, 726.

(6) Lara, K. O.; Godoy-Alcázar, C.; Rivera, I. L.; Eliseev, A. V.; Yatsimirski, A. K. *J. Phys. Org. Chem.* **2001**, 14, 453.

(7) Keehn, P. M., Rosenfeld, S. M., Eds. *Cyclophanes*; Academic Press: New York, 1983; Vols. 1 and 2.

(8) Diederich, F. *Cyclophanes: Monographs in Supramolecular Chemistry*; The Royal Society of Chemistry: London, 1991.

(9) Vogtle, F. *Cyclophane Chemistry*; Wiley: New York, 1983.

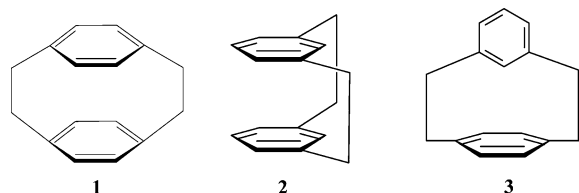


FIGURE 1. [2.2]Cyclophanes.

energies and bending angles are from semiempirical calculations.⁷ Transannular interactions have been probed by photoelectron and UV spectroscopy.⁹ NMR has been used to demonstrate transannular proton shieldings and transannular substituent effects.^{7–9} In comparison, vigorous, high-level theoretical studies that examine geometries, conformations, strain, and relative aromaticity are lacking.

The present study seeks to address these issues by analyzing the geometries, relative energies, aromaticity, strain imposed by the tether, NMR chemical shifts, and the atomic charges for compounds **1–3** employing various sophisticated computational methods. Relative stability order and tension at the ethano-bridges were examined for all isomers. Relative aromaticity in the [2.2]cyclophanes was gauged by using different criteria. Atomic charges and the NMR chemical shifts were also computed and compared.

2. Computational Methods

All electronic structure calculations were done by Gaussian 98 software.¹⁰ The geometry optimization was carried out by B3LYP,¹¹ B3PW91,¹² HF, and MP2¹³ methods employing 6-31G(d),¹⁴ 6-31+G(d,p),¹⁵ 6-31G(d;0.25) (standard d-functions on non-hydrogen atoms were replaced by more diffuse ones with exponents 0.25),¹⁶ and cc-pVDZ¹⁷ basis sets. For the analysis of the electron density, B3LYP/6-31+G(d,p) and B3PW91/6-31+G(d,p) models were used. MK,¹⁸ GAPT,¹⁹ which were calculated from the atomic polar tensors, extracted from the output of Gaussian 98 frequencies calculation, and

(10) Frisch, M. J.; Trucks, G. W.; Schlegel, H. B.; Scuseria, G. E.; Robb, M. A.; Cheeseman, J. R.; Zakrzewski, V. G.; Montgomery, J. A., Jr.; Stratmann, R. E.; Burant, J. C.; Dapprich, S.; Millam, J. M.; Daniels, A. D.; Kudin, K. N.; Strain, M. C.; Farkas, O.; Tomasi, J.; Barone, V.; Cossi, M.; Cammi, R.; Mennucci, B.; Pomelli, C.; Adamo, C.; Clifford, S.; Ochterski, J.; Petersson, G. A.; Ayala, P. Y.; Cui, Q.; Morokuma, K.; Malick, D. K.; Rabuck, A. D.; Raghavachari, K.; Foresman, J. B.; Cioslowski, J.; Ortiz, J. V.; Stefanov, B. B.; Liu, G.; Liashenko, A.; Piskorz, P.; Komaromi, I.; Gomperts, R.; Martin, R. L.; Fox, D. J.; Keith, T.; Al-Laham, M. A.; Peng, C. Y.; Nanayakkara, A.; Gonzalez, C.; Challacombe, M.; Gill, P. M. W.; Johnson, B. G.; Chen, W.; Wong, M. W.; Andres, J. L.; Head-Gordon, M.; Replogle, E. S.; Pople, J. A. *Gaussian 98*, revision A.7; Gaussian, Inc.: Pittsburgh, PA, 1998.

(11) Becke, A. D. *J. Chem. Phys.* **1993**, *98*, 5648.

(12) Perdew, J. P.; Burke, K.; Wang, Y. *Phys. Rev. B* **1996**, *54*, 16533.

(13) Frisch, M. J.; Gordon, M. H.; Pople, J. A. *Chem. Phys. Lett.* **1990**, *166*, 275.

(14) Petersson, G. A.; Al-Laham, M. A. *J. Chem. Phys.* **1991**, *94*, 6081.

(15) Petersson, G. A.; Tensfeldt, T. G.; AL-Laham, M. A.; Shirley, W. A.; Mantzaris, J. *J. Chem. Phys.* **1988**, *89*, 2193.

(16) Kroon-Batenburg, L. M. J.; Van Duijneveldt, F. B. *THEOCHEM* **1985**, *121*, 185.

(17) Woon, D. E.; Dunning, T. H., Jr. *J. Chem. Phys.* **1993**, *98*, 1358.

(18) Besler, B. H.; Merz, K. M., Jr.; Kollman, P. A. *J. Comput. Chem.* **1990**, *11*, 431.

(19) Cioslowski, J. *J. Am. Chem. Soc.* **1989**, *111*, 8333.

NPA²⁰ charges were tested. The chemical shifts were obtained by GIAO method.²¹ Aromaticity was calculated by NICS²² and HOMA.²³ NICS was calculated at the center of the ring, NICS(0), 1 Å above and 1 Å below this point, NICS(1) and NICS(-1), respectively. The variation of NICS with distance was also calculated. Conformational analysis of **2** and **3** was made by SUMM²⁴ and Low Mode Search²⁵ with MM3 force field.²⁶ Both search protocols produced similar results.

3. Results and Discussion

3.1. Molecular Structure of [2.2]Cyclophanes.

Since there are no high-level computational studies of [2.2]cyclophanes in the literature, it was necessary to do a study of the ability of different electronic structure models to reproduce the experimental geometry of these compounds. The most appropriate isomer to undertake this study is [2.2]paracyclophane **1**. Despite its rigid structure, the methylene bridges can present small distortions from the parallel arrangement to relieve steric repulsions, reducing the point group from D_{2h} to D_2 (Figure 2). For many years, these distortions have been a matter of debate among structural chemists. Recent theoretical data indicate that **1** present the D_2 point group.²⁷ However, some experimental data indicate that this system is disordered.²⁸ In addition, the aromatic rings are distorted away from planarity. It is interesting to judge the suitability of computational methods to describe both effects. By analysis of the bond lengths we can observe that the MP2/6-31G(d;0.25) level overestimates these variables (Tables S1–S4, Supporting Information). The results from other basis set are quite similar and are in good agreement with the experimental values. For the bond angles all methods presented values in good agreement with X-ray data.²⁸ In contrast, the dihedral angles of the ethano bridges, $C_1C_7C_7C_1$ and $C_4C_8C_8C_4$, are very dependent on the model. MP2 and B3PW91 methods with both 6-31G(d) and 6-31+G(d,p) basis sets and HF/cc-pVDZ provided structures with the correct symmetry. It is interesting to note that MP2 overestimates and B3LYP and HF methods underestimate the distortion of the bridge. This can indicate that MP2 overestimates the steric repulsion between hydrogen atoms in ethano bridges and the other methods underestimate it. Geometry optimizations using cc-pVDZ, for all methods, and MP2/6-31G(d;0.25) basis set result in D_{2h} structure and B3LYP produces a near eclipsed conformer.

The conformers for [2.2]metacyclophane **2** and [2.2]-metaparacyclophane **3** were obtained through conformational searching (Figure 3).

(20) Reed, A. E.; Weinstock, R. B.; Weinhold, F. *Chem. Phys.* **1985**, *83*, 735.

(21) Ditchfield, R. *Mol. Phys.* **1974**, *27*, 789.

(22) Schleyer, P. V. R.; Maerker, C.; Dransfeld, A.; Jiao, H.; Hommes, N. J. R. *J. Am. Chem. Soc.* **1996**, *118*, 6317.

(23) Krygowski, T. M.; Cyrański, M. K.; Czarnocki, Z.; Häfelinger, G.; Katritzky, A. R. *Tetrahedron* **2000**, *56*, 1783.

(24) Goodman, J. M.; Still, W. C. *J. Comput. Chem.* **1991**, *12*, 1110.

(25) Kolossváry, I.; Guida, W. C. *J. Am. Chem. Soc.* **1996**, *118*, 5011.

(26) Allinger, N. L.; Yuh, Y. H.; lii, J. H. *J. Am. Chem. Soc.* **1989**, *111*, 8551.

(27) Henseler, D.; Hohlneicher, G. *J. Phys. Chem. A* **1998**, *102*, 10828.

(28) Hope, H.; Bernstein, J.; Trueblood, K. N. *Acta Crystallogr., Sect. B* **1972**, *28*, 1733.

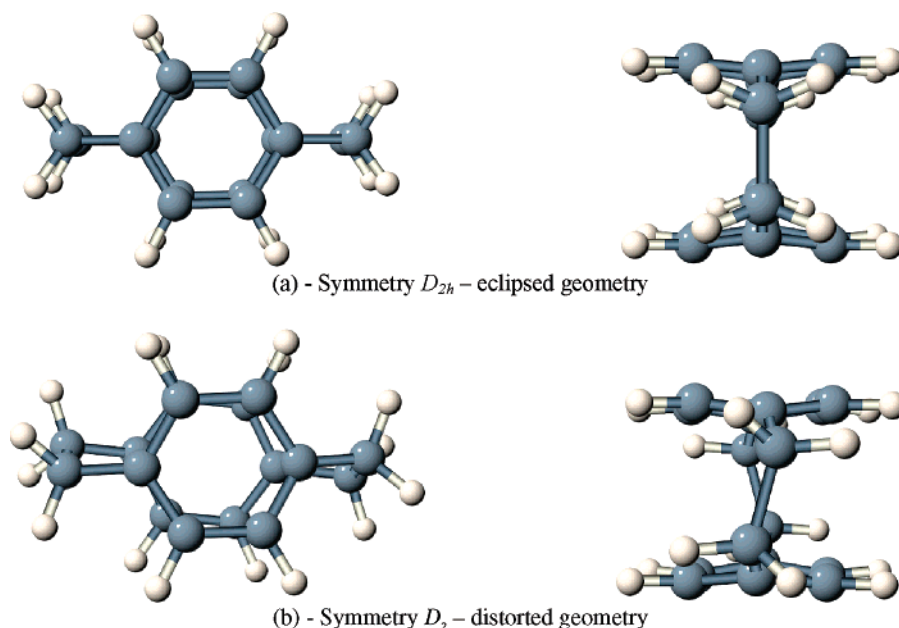


FIGURE 2. Top and side views of eclipsed (D_{2h}) and distorted (D_2) geometries of [2.2]paracyclophane.

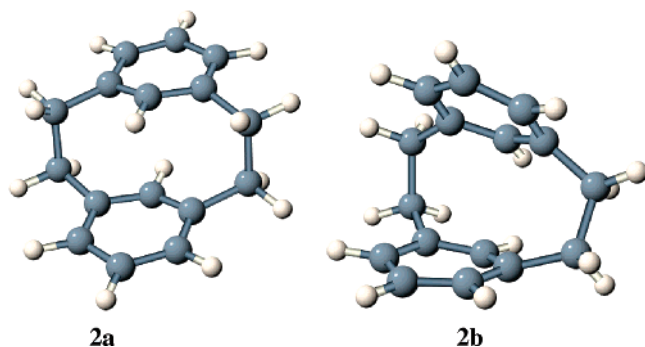


FIGURE 3. Conformers of [2.2]metacyclophane **2**.

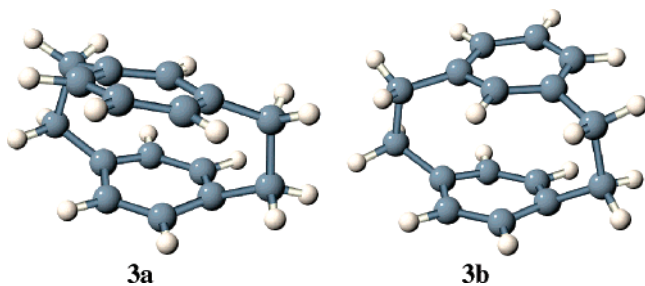


FIGURE 4. Conformers of [2.2]metaparacyclophane, **3**.

Two conformers were obtained for isomer **2**: **2a**, named *anti*-[2.2]metacyclophane, is the most stable, with a steric energy around $150.0 \text{ kJ}\cdot\text{mol}^{-1}$. The less stable conformer, **2b**, *syn*-[2.2]metacyclophane, presents a steric energy around $200.5 \text{ kJ}\cdot\text{mol}^{-1}$. These steric energy values were obtained by using the MM3 force field. The lower stability can be attributed to the repulsive interaction between the aromatic clouds as a result of stacking. Isomer **3** presents only two degenerate conformers, **3a** and **3b** (Figure 4).

According to these results, there are two conformers, **2a** and **2b**, for isomer **2** and a unique conformer, **3a**, for isomer **3**. The geometric parameters of these conformers

were calculated using the combinations B3LYP/6-31+G(d,p), B3PW91/6-31+G(d,p), and MP2/6-31+G(d,p). The choice of these methods is justified by the fact that they provided good geometry results for the isomer **1**. The model MP2/6-31G(d;0.25) was also tested for these conformers to explore the effect of polarization functions on the descriptions of the geometric parameters of the large molecules.

Tables S1, S2, and S3 summarize the calculated and experimental^{29,30} geometric parameters of the conformers **1**, **2a**, and **2b**, respectively (Supporting Information). B3PW91 functional gave better CC distances than those from B3LYP or MP2, and MP2/6-31G(d;0.25) had a tendency to overestimate CC distances. The CH distances were overestimated by both DFT methods and MP2/6-31G(d;0.25). The MP2/6-31+G(d,p) calculations provided better values of the bond angles than the other methods. For these conformers, B3PW91/6-31+G(d,p) and MP2/6-31+G(d,p) models present the best agreement with experimental geometric parameters.

The same treatment was used to evaluate the geometrical parameters of the conformer **3a**. In this case, only data concerning the CC bond lengths and bond angles are presented because experimental values for CH distances could not be found. The results summarized in Table S4 (Supporting Information) show that the methods B3PW91/6-31+G(d,p) and MP2/6-31+G(d,p) computed smaller bond lengths than B3LYP/6-31+G(d,p) and MP2/6-31G(d;0.25) methods. Furthermore, we can observe that MP2/6-31G(d;0.25) is a poor choice for routine calculations of cyclophane structures because it overestimates all bond lengths. Despite these results, we can also observe that the calculated bond angles are less sensitive to methods and basis set changes. Again, the best models are B3PW91/6-31+G(d,p) and MP2/6-31+G(d,p).

(29) Yasushi, K.; Yasuoka, N.; Kasai, N. *Acta Crystallogr., Sect. B* **1977**, *33*, 754.

(30) Champion, R.; Godfrey, P. D.; Bettens, F. L. *J. Mol. Spectrosc.* **1992**, *155*, 18.

TABLE 1. Statistical Analyses of CC Bond Lengths for the [2.2]Cyclophanes (Å)^a

method/basis set	MD	MPE	MNE	mean	σ
1					
B3LYP/6-31+G(d,p)	0.015	0.018	-	1.400	0.016
B3PW91/6-31+G(d,p)	0.013	0.016	-	1.400	0.015
MP2/6-31+G(d,p)	0.016	0.019	-	1.390	0.021
MP2/6-31G(d;0.25)	0.037	0.039	-	1.420	0.008
2a					
B3LYP/6-31+G(d,p)	0.058	0.143	-0.041	1.448	0.056
B3PW91/6-31+G(d,p)	0.057	0.134	-0.043	1.444	0.062
MP2/6-31+G(d,p)	0.053	0.127	-0.040	1.444	0.052
MP2/6-31G(d;0.25)	0.047	0.153	-0.019	1.466	0.069
2b					
B3LYP/6-31+G(d,p)	0.004	0.006		1.430	0.001
B3PW91/6-31+G(d,p)	0.002	0.003		1.427	0.001
MP2/6-31+G(d,p)	0.005	0.007		1.428	0.001
MP2/6-31G(d;0.25)	0.026	0.027		1.422	0.001
3a					
B3LYP/6-31+G(d,p)	0.058	0.149	-0.043	1.449	0.068
B3PW91/6-31+G(d,p)	0.058	0.140	-0.045	1.445	0.066
MP2/6-31+G(d,p)	0.054	0.133	-0.041	1.446	0.062
MP2/6-31G(d;0.25)	0.047	0.160	-0.021	1.468	0.063
All					
B3LYP/6-31+G(d,p)	0.056	0.180	-0.040	1.463	0.243
B3PW91/6-31+G(d,p)	0.055	0.168	-0.042	1.459	0.242
MP2/6-31+G(d,p)	0.051	0.152	-0.038	1.460	0.241
MP2/6-31G(d;0.25)	0.044	0.191	-0.018	1.481	0.245

$${}^a MD = \frac{\sum_{i=1}^n |d_{i(\text{calc})} - \langle d_{\text{exp}} \rangle|}{n}; AD = \Delta d = d_{\text{calc}} - \langle d_{\text{exp}} \rangle, MPE = \max AD, MNE = \min AD.$$

A statistical analysis of the ability for each method to reproduce CC bond lengths was performed for each [2.2]-cyclophane **1**, **2a**, **2b**, and **3a** and for all compounds (Table 1).

According to Table 1, the quality of bond lengths calculated by B3LYP/6-31+G(d,p), B3PW91/6-31+G(d,p), and MP2/6-31+G(d,p) models are similar. On the other hand, MP2/6-31G(d;0.25) frequently presents larger errors. Nevertheless, the geometries calculated by hybrid DFT methods and basis sets with diffuse and polarization functions present good results for [2.2]cyclophanes. The obtained results are in close agreement with results reported in the literature, which apply some DFT methods for large and symmetrical molecules.³¹

3.2. Energies. Table 2 summarizes the relative energies for various [2.2]cyclophane conformers. All attempts to calculate the MP2 frequencies were unsuccessful.

Table 2 indicates that order of stability is the same for all methods and it is not changed by ZPE, **2a** > **3a** > **2b** > **1**. The larger stability of the conformer **2a** is related to the parallel displacement conformation of the aryl rings, which minimizes electronic repulsion between the π electronic clouds. Conformer **1** has a low stability due to intense electronic repulsion between aromatic rings. This intense repulsion can also be noted via distortion of planarity of the aryl rings. The conformers **3a** and **2b** have an intermediate stability that is justified by spatial displacement of the aromatic rings. These conformers also have distorted aryl rings but this distortion is smaller than that observed in conformer **1**. Theoretical studies indicate that the most stable conformations for

TABLE 2. Electronic Energies (E), Zero-Point Correction (ZPE), and Total Energy (Hartree) and Relative Energies, ΔE (kcal/mol), for [2.2]Cyclophanes

conformers	E	ZPE	$E + ZPE$	ΔE
B3LYP/6-31+G(d,p)				
1	-619.3426021	0.273428	-619.069174	19.81
2a	-619.3764982	0.275753	-619.100746	0.00
2b	-619.3585782	0.274272	-619.084306	10.32
3a	-619.3601063	0.274284	-619.085822	9.36
B3PW91/6-31+G(d,p)				
1	-619.1073766	0.274267	-618.833109	20.58
2a	-619.1417279	0.275815	-618.865912	0.00
2b	-619.123083	0.275012	-618.848071	11.20
3a	-619.1255004	0.275023	-618.850477	9.68
MP2/6-31+G(d,p)				
1	-617.3959223		-617.3959223	17.85
2a	-617.4243725		-617.4243725	0.00
2b	-617.4073738		-617.4073738	10.67
3a	-617.4144263		-617.4144263	6.24
MP2/6-31G(d;0.25)				
1	-616.8375365		-616.8375365	17.00
2a	-616.8646429		-616.8646429	0.00
2b	-616.8476648		-616.8476648	10.65
3a	-616.8556276		-616.8556276	5.66

benzene dimer have parallel displaced and a perpendicular arrangement of the rings.³²

3.3. Isodesmic Reactions. The energy of the cleavage of ethano bridges, via isodesmic reactions, was used as a way to evaluate transannular interaction between the aromatic rings and the strain induced by the tether. Isodesmic reactions have been regularly applied to evaluate strain in cyclic organic compounds.³³ Table 3 presents the strain energies obtained through isodesmic reactions SE(IR) and the energy differences (ΔE) among the isomers, corrected by zero-point energy, calculated by the B3PW91/6-31+G(d,p) model.

The SE(IR) values indicate that the ethano bridges in conformer **1** are most strained. The less strained conformer is **2a**, which has the aryl rings in opposite positions. It is also interesting to note that conformers **2b** and **3a** have similar tensions on the ethano bridges. This similarity can be attributed to the fact that these conformers have similarity in the relative arrangement of the aryl rings (Figures 3 and 4). Relative energies for the isodesmic reactions SE(IR) follow the same order as the relative energies (ΔE) (Tables 2 and 3) indicating that the repulsion of aromatic rings and strain imposed via ethano bridges are the main factors that determine the stability of [2,2]cyclophanes. To separate the deformations on bond lengths and nonbonded interactions that affect the strain energies in the above-mentioned approach, a partitioned treatment of the strain energies were considered.³⁴ In this approach, cyclophane bridges were disconnected while the structure of benzene rings were maintained in the original geometry. The free valencies of the rings were filled with hydrogen atoms. Separated single point calculations were performed on both the dimer benzene and the bridges, maintaining both in the conformations of the corresponding cyclo-

(32) Jennings, W. B.; Farrel, B. M.; Mslone, J. F. *Acc. Chem. Res.* **2001**, *34*, 885.

(33) Wiberg, K. B. *Angew. Chem., Int. Ed. Engl.* **1986**, *25*, 312.

(34) Eiss, M. J. V.; Wolf, W. H.; Bickelhaupt, F.; Boese, R. *J. Chem. Soc., Perkin Trans. 2* **2000**, 793.

(31) Pascal, R. A., Jr. *J. Chem. Phys. Chem. A* **2001**, *105*, 9040.

TABLE 3. Isodesmic Reactions

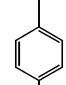
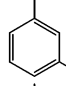
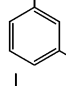
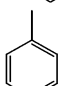
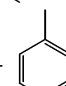
Isodesmic reactions			SE(IR) (kcal/mol)	ΔE (kcal/mol)
(1) + 4 CH ₄	\longrightarrow	2  + 2 CH ₃ —CH ₃	-29.72	20.58
(2a) + 4 CH ₄	\longrightarrow	2  + 2 CH ₃ —CH ₃	-9.27	0.00
(2b) + 4 CH ₄	\longrightarrow	2  + 2 CH ₃ —CH ₃	-20.46	11.20
(3a) + 4 CH ₄	\longrightarrow	 +  + 2 CH ₃ —CH ₃	-18.90	9.68

TABLE 4. Strain Energies (SE/kcal mol⁻¹) and Partitioning in Different Components (kcal mol⁻¹)

compd	SE(IR)	SE(bb)	anti				eclipsed			
			SE(br-a)	SE(rep-a)	SE(sum-a)	SE(bb)/SE(Sum-a)	SE(br-e)	SE(rep-e)	SE(sum-e)	SE(bb)/SE(Sum-e)
1	29.72	17.85	25.90	14.03	43.75	0.408	14.54	2.67	32.39	0.551
2a	9.27	5.88	16.74	13.35	22.62	0.260	5.26	1.87	11.14	0.528
2b	20.46	6.40	21.05	7.00	27.45	0.233	9.56	-4.50	15.96	0.401
3a	18.90	9.83	20.53	11.46	30.36	0.323	9.05	-0.02	18.88	0.521

phanes. The obtained energy values were compared with the energy of optimized reference compounds, e.g., benzene dimer (maintaining frozen the distance between benzene rings) and butane in two different conformations *anti* (a) and *eclipsed* (e). These differences provided the steric energies of the bent benzene dimer SE(bb) and of the bridges SE(br). The SE(br) was partitioned in two different terms according to the conformation of the butane, SE(br-a) denotes the strain energy of bridges obtained by using the anti conformer of butane and SE(br-e) denotes the strain energy of bridges obtained by using the eclipsed conformer of butane. The sum of these component values, SE(bb) and SE(br-a) or SE(br-e) is denoted SE(sum). According to Table 4, the SE(bb) values are smaller than the SE(br-a), which means that the changes in bridges energy by torsion are large, while the rings are considered more rigid, (Tables S1–S4, Supporting Information). However, when we consider the eclipsed conformation of butane the results are opposite, the SE(bb) values are larger than SE(br-e), indicating that the aromatic rings absorb more strain than the ethano bridges, when these bridges are in a conformation similar to the one observed in cyclophanes. It can be concluded that the decks are absorbers of strain energy, as observed by Eis and co-workers.³⁴

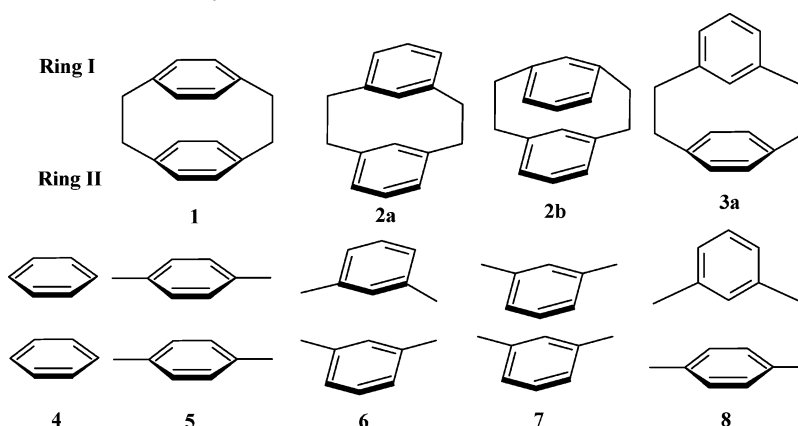
The repulsive nature of the interactions between rings and bridges is computed by the component SE(rep), which is the difference between SE(sum) and SE(IR). Considering the anti conformation (a), the SE(rep-a) values are similar for the isomers **1**, **2a**, and **3a**, but **2b** presents the smallest value of SE(rep-a), which suggests an inversion in the stability order of **2b** and **3a** when the values of SE(sum-a) and SE(IR) are compared. In addition, the values of SE(rep-e) showed the same trend as of SE(rep-a), however, with values smaller than the later, indicating very small repulsion in the bridge considering

e-butane as a reference. The order of stability (Table 3) is correlated with the partitioned steric energies SE(bb) and SE(br), **1** has the largest values of SE(bb) and SE(br), which shows that **1** is the most tensioned system. On the other hand, **2a**, **2b**, and **3a** present small values of SE(bb) but large values of SE(br-a), indicating that the bridges are more strained than the rings when the anti conformer is considered in the calculation. In contrast, when *eclipsed* conformer is considered in the calculation, we can observe that the rings absorb more strain than the ethano bridges. The coefficient SE(bb)/SE(sum) provided additional information about the distribution of SE. According to the SE(bb)/SE(sum-a) values, the rings of **1** and **3a** support more tension than the rings of **2a** and **2b**. However, considering the *eclipsed* conformation (e), SE(bb)/SE(sum-e) indicates that the strain supported by the rings is similar in all isomers and the ring **1** is most strained than the others. Summarizing, two different results can be reported. When the *anti* conformation of butane (a) is considered to determine SE(Br), the results suggest that the bridges can support more tension than the rings, but when the *eclipsed* conformation of butane (e) is considered, the results present close agreement to those observed for cyclophane systems with large bridges and only one ring, which suggest that the rings can absorb more tension than the bridges.³⁴

3.4. Aromaticity. Aromaticity was calculated by two different criteria, NICS and HOMA. The former is a measure of magnetic aromaticity, and the components of the last, EN and GEO, are related with energetic and geometric changes in aromaticity.^{35,36} NICS was computed for the [2.2]cyclophanes, for benzene, *p*-xylene,

(35) Cyrański, M. K.; Krygowski, T. M. *Chem. Rev.* **2001**, *101*, 1385.(36) Schleyer, P. V. R.; Maerker, C.; Dransfeld, A.; Jiao, H.; van Eikema Hommes, N. J. R. *J. Am. Chem. Soc.* **1996**, *118*, 6317.

TABLE 5. NICS (ppm) for the Aromatic Systems



compd	ring I			ring II		
	NICS(0)	NICS(out)	NICS(in)	NICS(0)	NICS(out)	NICS(in)
benzene	-8.24	-10.39	-10.39			
<i>p</i> -xylene	-8.24	-9.93	-9.93			
<i>m</i> -xylene	-8.26	-9.95	-9.95			
1	-8.71	-9.56	-12.90	-8.71	-9.56	-12.90
2a	-8.79	-9.58	-11.14	-8.70	-9.58	-11.13
2b	-9.03	-9.42	-13.25	-8.90	-9.47	-13.37
3a	-10.31	-10.70	-14.28	-9.70	-9.17	-15.25
4	-7.53	-10.62	-9.35	-7.49	-10.55	-9.38
5	-6.92	-10.16	-7.68	-7.20	-10.42	-7.90
6	-7.08	-9.09	-8.27	-7.05	-9.04	-8.32
7	-7.26	-10.15	-8.33	-7.35	-10.35	-8.60
8	-10.13	-10.80	-14.41	-10.80	-10.98	-15.20

m-xylene, and the stacked dimers of these molecules. In these dimers, the relative position of aromatic rings was similar to cyclophanes. To avoid confusion, instead of the common nomenclature of NICS(1) and NICS(-1), NICS(out) and NICS(in) was used to refer to NICS calculated at a distance of 1 Å from the ring center and directed outside and inside the cavity created by the cyclophane rings, respectively. For NICS of a specific ring, the notation adopted is NICS(in/out, ring). For example, NICS(in,I) is NICS(in) for ring I. Results for density functionals B3PW91 and B3LYP with 6-31+G(d,p) basis set are qualitatively similar and only the first is presented (Table 5).

Only NICS(in) and NICS(out) were analyzed because they are more appropriate to evaluate the aromaticity in the six-membered rings than NICS(0).^{37,38} The stacking of two benzenes or two xylenes in **4**, **5**, and **7** leads to an increase in NICS(out) and a decrease in NICS(in). For **6** and **8**, both NICS values decrease on dimer formation. This difference can be ascribed to the fact that phenyl rings in dimers **6** and **8** are displaced and the interaction between the aromatic rings is not as strong as in the other dimers. Both NICS(in) and NICS(out) decrease with dimethyl substitution in each ring of **4**. A comparison of NICS for xylenes with corresponding cyclophanes indicate that the bridging process decreases NICS(in) for **5**–**7**. Both NICS(in) for **8** remain constant, as NICS(out,I) for this compound. NICS(out) increases for **3a**, **2b** and ring II of **8**. As a decrease of NICS indicates an increase

in the electronic density, apart from the effects of neighbor groups, Δ NICS values suggest an increase in the electronic density in the inner portion of benzene and xylenes dimers when the rings are stacked. Bridges induce an additional increase in the electronic density. The outer portion of the dimers presents a depletion of electronic density. These conclusions are in contrast with an AIM study of cyclophanes.³⁹

To explore these observations in depth, NICS was computed for points perpendicular to the center of the rings, for [2.2] paracyclophane **1**, and for the dimers **4** and **5** (Figure 5). Outside the rings the behavior all three compounds is similar; the curves for **4** and **5** are coincident and **1** presents slightly larger values than the latter. In the cavity between the rings, there are very large changes in NICS behavior: **5** is larger and **1** is much smaller than **4**. This can indicate that there is a decrease in electronic density inside both rings, from **4** to **5**, and a large increase in the bridging process. These results agree with those observed in superphanes, which suggest that the electron delocalization is not only on the rings but also in the whole molecule.⁴⁰ It is also curious to observe that in three systems there is a small increase of NICS in the center of the cavity. This suggests that the electronic density is more concentrated near the rings and decreases from one ring to another.

In addition, NICS_{zz}, the component of NICS tensors corresponding to the principal axis perpendicular to the ring plane (*z*-axis) was analyzed. NICS_{zz} was found to be

(37) Schleyer, P. V. R.; Manoharan, M.; Wang, Z.; Kiran, B.; Jiao, H.; Puchta, R.; Hommes, N., J., R., E. *Org. Lett.* **2001**, *16*, 2465.

(38) Schulman J. M.; Disch, R. L.; Jiao, H.; Schleyer, P. v. R. *J. Phys. Chem. A* **1998**, *102*, 8051.

(39) Bader, R. F. W. *Atoms in Molecules: A Quantum Theory*; Clarendon: Oxford, 1990.

(40) Mireles, N.; Salcedo, R.; Sansores, L. E.; Martínez, A. *Int. J. Quantum Chem.* **2000**, *80*, 258.

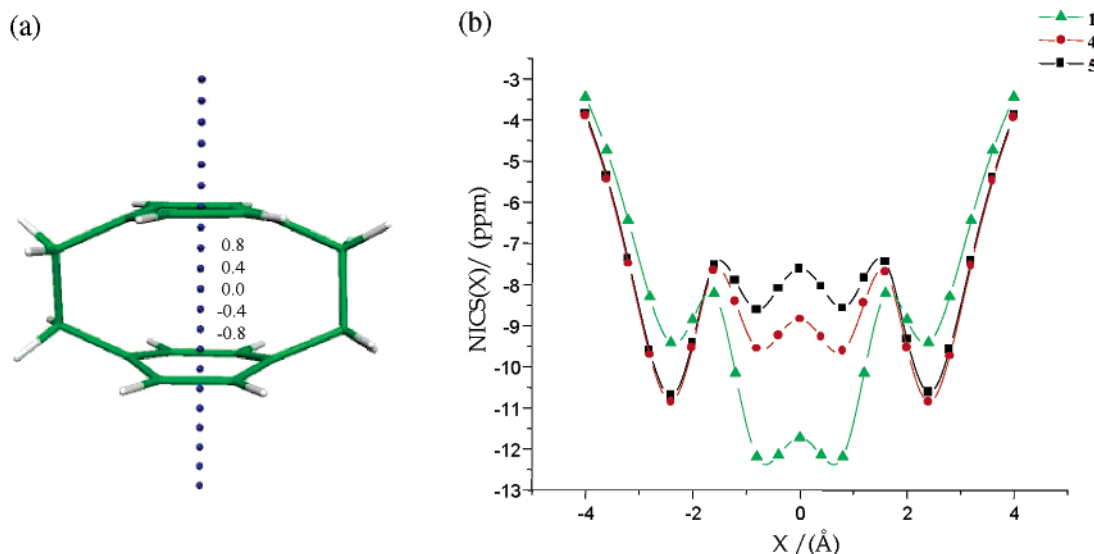


FIGURE 5. (a) Point distribution for NICS plots. (b) NICS plot for **1**, **4**, and **5**.

TABLE 6. NICS (ppm) and the Component of NICS Tensor (NICS_{zz}) (ppm)

compd	d (Å)	NICS	NICS_{zz}
benzene	0	-8.2	-13.6
1	1	-10.4	-29.0
1 (ring I)	0	-8.3	-20.9
	1 (out)	-9.6	-28.9
2a (ring I)	-1 (in)	-12.9	-46.1
	0	-7.1	-14.3
2a (ring I)	1 (out)	-9.1	-25.0
	-1 (in)	-8.3	-27.1
2b (ring I)	0	-7.3	-14.3
	1 (out)	-10.2	-25.0
2b (ring I)	-1 (in)	-8.3	-27.2
	0	-11.0	-16.2
3a (ring I)	1 (out)	-10.8	-24.3
	-1 (in)	-14.4	-31.9
3a (ring II)	0	-10.8	-17.9
	-1 (out)	-11.0	-25.3
	1 (in)	-15.2	-40.7

a good measure for the characterization of the π system of a ring.⁴¹ For [2.2]cyclophanes, NICS_{zz} can characterize better the π systems than the isotropic NICS because NICS_{zz} corresponds more directly to the induced current densities in molecular rings. The NICS tensor contributions were computed along the z -axis, at the ring center, and at 1.0 Å above (+1) and below (-1) from the $z = 0$ plane.

According to Table 6, the values of $\text{NICS}_{zz}(0)$ present large differences from one isomer to another because NICS in the plane of rings is affected by the σ framework. The NICS_{zz} values are similar for **2a** and **2b**. On the other hand, the $\text{NICS}_{zz}(\text{in})$ of **1** and **3a** is larger than $\text{NICS}_{zz}(\text{in})$ of **2a** and **2b**, indicating an increase of the aromaticity for these systems. The values of $\text{NICS}_{zz}(\text{out})$ are similar for all isomers (25.0 ppm), indicating an equivalent behavior outside the ring, according to data reported before (Figure 5 and Table 5). Despite the fact that NICS values indicate that there is an increase of the electronic density inside the [2.2]cyclophanes cavity, the NICS_{zz}

TABLE 7. HOMA, EN, and GEO for the Aromatic Systems

compd	ring I			ring II		
	HOMA	EN	GEO	HOMA	EN	GEO
benzene	0.978	0.021	0.000			
<i>p</i> -xylene	0.972	0.025	0.003			
<i>m</i> -xylene	0.976	0.022	0.001			
1	0.945	0.053	0.003	0.945	0.053	0.003
2a	0.972	0.028	0.001	0.972	0.028	0.001
2b	0.966	0.033	0.001	0.966	0.033	0.001
3a	0.966	0.032	0.001	0.969	0.031	0.001

values not only suggest a general increase of the aromaticity to these systems but also indicate that the increase of density is predominantly inside of the cavity of **1** and **3a** ($\text{NICS}_{zz}(\text{in}) = -46.1, -31.9, -40.7$), respectively.

HOMA and its components EN and GEO were calculated using geometries optimized by B3PW91, B3LYP, and MP2 methods with the 6-31+G(d,p) basis set. Since these methods present the same qualitative trends, only results for the first are presented in Table 7. HOMA is determined by EN, as GEO is nearly zero for all compounds. This indicates that C–C bonds in the aromatic rings are smaller or larger than the standard value proposed in the method and there is no significant bond alternation, as it can be observed in bond length tables (Tables S1–S4, Supporting Information). Despite the fact that the aromatic rings are in the boat conformation, all [2.2]cyclophanes are aromatic. The aromaticity follows the stability order, indicating that in-plane and out-of-plane deformation contributes to the stability of these compounds.

3.5. Atomic Charges. The atomic charges obtained through the MK, NPA, and GAPT methods are shown in Table S9 (Supporting Information). For the B3LYP/6-31+G(d,p) model all charges for ring carbons isomer **1** are negative. For the ethano bridges, NPA and GAPT are negative and MK carbon charges are positive. For **2a**, **2b**, and **3a**, MK and GAPT presented negative charges for ring carbons. In contrast, NPA predict that charges in these atoms are negative and positive charges for bridge carbons. Only MK carbon bridge charges are negative.

(41) Corminboeuf, C.; Heine, T.; Seifert, G.; Schleyer, P. v. R.; Weber, J. *Phys. Chem. Chem. Phys.* **2004**, *6*, 273

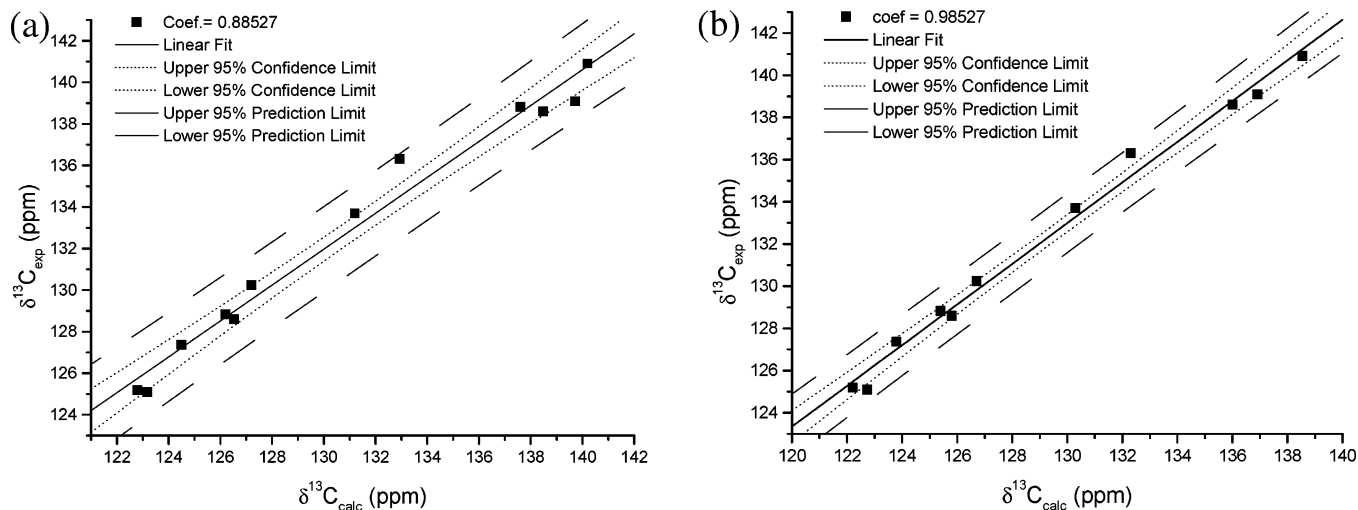


FIGURE 6. Linear dependence between calculated and experimental ^{13}C chemical shifts of rings for isomers: (a) B3LYP/6-31+G(d,p) and (b) B3PW91/6-31+G(d,p).

3.6. Chemical Shifts. The chemical shifts were calculated at the B3LYP/6-31+G(d,p) and B3PW91/6-31+G(d,p) levels of theory. These shifts were determined by computing the difference between the absolute magnetic shielding of [2.2]cyclophanes atoms and TMS as standard reference. Table S10 (Supporting Information) presents the experimental and B3PW91/6-31+G(d,p) proton and carbon chemical shifts for isomers, **1**, **2a**, and **3a**, as experimental chemical shifts for **2b** are not found in the literature. Mitchell⁴¹ and co-workers suggested that the *syn* form (**2b**) changes to the *anti* form (**2a**) with a small increase of the temperature. This method presents a better linear correlation with experimental data for ^{13}C chemical shifts than B3LYP/6-31+G(d,p) (Figure 6). All calculated chemical shifts are in good agreement with the experimental values.^{42–44}

In general, the carbons located at benzene rings appear at higher frequencies for **1** than **2a** and **2b**. The carbons located at the ethano bridges of **2a** are more shielded than the carbons of the other isomers. In relation to the chemical shifts of the hydrogen atoms, the ring protons in **1** and **3a** are more shielded than those of **2a**. The protons located at ethano bridges in **2a** and **3a** are more shielded than the bridge protons in **1**. These results suggest that the diamagnetic anisotropy is more intense in **1** than in the other isomers.

4. Conclusions

Geometry optimization predict a D_2 structure for [2.2]-paracyclophane **1**, two conformers (**2a** and **2b**) for [2.2]-metacyclophane **2**, and a unique conformer for [2.2]-metaparacyclophane **3**. The best geometries were calculated by MP2/6-31+G(d,p), B3LYP/6-31+G(d,p), and B3PW91/6-31+G(d,p) models. Isodesmic reactions for cleavage of ethano bridges and relative energies gave the same ordering, indicating that the two main factors that determine the stability are the repulsion of aromatic

clouds and the strain imposed by the ethano bridges. The partitioning treatment of strain energy applied to [2.2]-cyclophanes suggests that when the *anti* conformation of butane (a) is considered to determine SE(Br), the bridges can support more tension than the rings, but when the *eclipsed* conformation of butane (e) is considered, the rings can absorb more tension than the bridges. Aromaticity, described by NICS, suggests an increase of electron density inside the rings by stacking in benzene and xylene; an additional increase is observed upon the bridging process. In addition, NICS_{zz}(in) values indicated that the predominant increase of electron density occurs in the cavity of **1** and **3a**. HOMA is determined either by EN or shrinking and enlargement of C–C bonds from the standard values. HOMA decreases in the same way as stability, indicating a contribution of out-of-plane or in-plane ring deformations to the stability of [2,2]cyclophanes.

An analysis of atomic charges permits us to conclude that there is charge delocalization between the aromatic portions and the ethano bridges. The MK and GAPT charges show that electron density is concentrated at the carbons of the benzene rings. However, the NPA charges show that the carbons at the ethano bridges have negative charges. The computed chemical shifts are in good agreement with the experimental values. The results suggest that diamagnetic anisotropy is more intense in **1** than in the other isomers. Therefore, these values provide a good tool with which to analyze substitutions effects on electronic density.

Acknowledgment. We acknowledge the Brazilian foundations FAPESP, CAPES, and CNPq for financial support and LCCA-USP for the generous allocation of computer resources. S.E.G. thanks CNPq for a research scholarship (Grant No.301957/88-6), and G.F.C thanks FAPESP for a Ph.D scholarship (Grant No. 02/03753-5).

Supporting Information Available: Table S1: Theoretical and experimental geometry parameters of **1**. Table S2: Theoretical and experimental geometry parameters of **2a**. Table S3: Theoretical and experimental geometry parameters of **2b**. Table S4: Theoretical and experimental geometry

(42) Mitchell, R. H.; Vinod, T. K.; Bushnell, G. W. *J. Am. Chem. Soc.* **1990**, *112*, 3487.

(43) Laali, K. K.; Houser, J. J.; Filler, R.; Kong, Z. *J. Phys. Org. Chem.* **1994**, *7*, 105.

(44) Renault, A.; Cohen, A. C.; Lajzerowicz, B. *J. Acta Crystallogr.* **1987**, *B43*, 480.

parameters of **3a**. Tables S5–S8: Cartesian coordinates of the optimized structure for **1**, **2a**, **2b**, and **3a** by MP2/6-31+G(d,p), respectively. Table S9: MK, NPA, and GAPT charges for isomers **1**, **2a**, **2b**, and **3a**. Table S10: Chemical shifts (ppm)

for the isomers **1**, **2a**, **2b** and **3a**. This material is available free of charge via the Internet at <http://pubs.acs.org>.

JO047864D